

Ground-to-space bistatic radar measurements of auroral irregularities with RAX

Hasan Bahcivan¹, James Cutler², John Springman², Rick Doe¹

The second Radio Aurora Explorer (RAX) satellite completed more than two dozen experiments with the AMISR chain of incoherent scatter radars in Gakona and Poker Flat, Alaska, and Resolute Bay, Canada. Coherent radar echo occurred during four of the passes: three during F region ion drifts of 700, 1000, and 1600 m/s, and one during artificial HF heating of the ionosphere by the HAARP heater. Following inspection of the summary range-time-intensity plots, segments of 1 MHz raw I & Q data containing the echoes were downloaded for high resolution scattered power and Doppler velocity measurements. An autocorrelation analysis and the application of a de-convolution algorithm mapped the distribution of E region backscatter with 3 km resolution in altitude and 0.1° in magnetic aspect angle. To our knowledge, these are the highest resolution UHF radar measurements made in the auroral region. We find that (1) out of the two dozen experiments, backscatter was observed when the electric was above a threshold near the ion acoustic speed (2) the measured phase velocity is given by the ion acoustic speed times the cosine of the flow angle ($C_s \cos \theta$), (3) the magnetic aspect angle distribution is single-peaked, (4) narrows down with increasing altitude to about -0.1° at 110 km, and (5) the mean aspect angle varies with altitude, the variation is due to the modification of the total magnetic field by the electrojet Hall current.

1. Introduction

Radio Aurora Explorer (RAX) is the first CubeSat funded by the NSF CubeSat-based Space Weather program. It is jointly conducted by SRI International and University of Michigan. The mission is a ground-to-space bi-static radar experiment designed to investigate field-aligned irregularities (FAI) of electron density driven by various plasma instabilities. Previously, FAI measurements have been obtained using ground-based coherent scatter radars. However, due to near vertical magnetic field line geometry at high-latitudes, it has been difficult to achieve scatter perpendicularity. The unique radar scattering geometry of a RAX experiment, composed of a transmitter on the ground and an orbiting receiver in space, enables unique high-resolution measurements of FAI.

The RAX II satellite (shown in Figure 1) was launched on 28 October 2011 from Vandenberg Air Force Base to a 104° inclination, elliptical orbit (400–820 km). The launch was provided by NASA's Educational Launch of Nanosatellites (ELaNa) program. As of Dec 4, 2012, RAX-2 completed 26 experiments with the AMISR chain of incoherent scatter radars in Gakona and Poker Flat, Alaska, and Resolute Bay, Canada. Coherent radar echo occurred during four of the passes: three during F region ion drifts of 700, 1000, and 1600 m/s, and one during artificial HF heating of the ionosphere by the HAARP heater. After on-board computing that lasts ~1h, the 1.2 GB of raw I and Q data are finally converted to a post-compression 50 KB RTI image and downloaded. See Figure 1 for the summary plots. Here we present the results from the experiment during the magnetic storm of March 8, 2012.

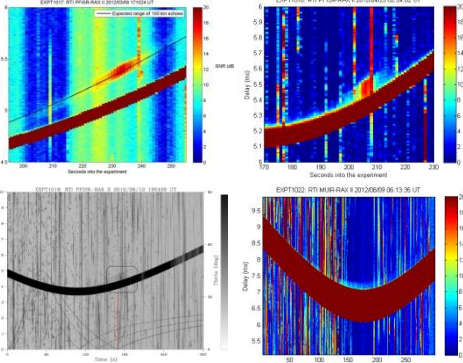


Figure 1: A total of 26 experiments conducted and data fully processed on board. 23 with natural irregularities, 3 with artificial irregularities produced by HAARP. Echoing occurred during 4 passes, including one with HAARP.

2. Experiment description

Figure 2 shows the loci-of-perpendicularity for the satellite altitude of 800 km and the satellite track shown by the dashed black line. The RAX radar receiver was turned on for 300s over the experimental zone, starting at 17:10:24 UT on 8 March 2012, collecting 14-bit I and Q samples at a rate of 1 MSPS each.

PFISR transmitted pulses in six beam directions. The beam dedicated to RAX reception of backscatter was pointed at 20.8° east of north and at 58° elevation, sending 100ms uncoded pulses at 449 MHz every 10ms. Halfway between the 100ms pulses for RAX, 480ms long pulses were transmitted to diagnose the background ionosphere using the incoherently scattered signals.

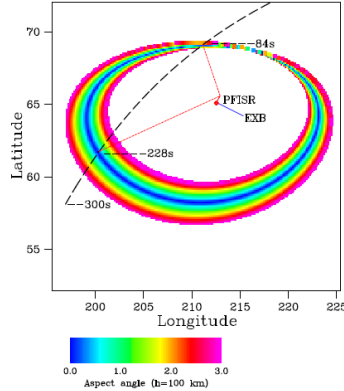


Figure 2: Experimental geometry showing the loci of perpendicularity at the spacecraft altitude (colored rings), spacecraft trajectory (dashed line), the incoming and scattered radar wave direction (thin red lines). Finally, the blue vector shows the direction of the EXB drift during the pass.

In the several weeks following this experiment, the raw I and Q data corresponding to the 235th second (at the original 1 MHz rate) was also downloaded for Doppler analysis. To measure the Doppler velocity of FAI, we computed the ACF lag at 90ms delay. This ACF was computed from 98 I and Q records corresponding to the 235th second (2 were manually excluded). We first computed the Doppler shift of the direct pulse from PFISR and applied a small frequency offset, Δf , to match to the Doppler shift corresponding to the projection velocity of the spacecraft along the PFISR line-of-sight, which was obtained from the ephemeris provided by North American Aerospace Defense command (NORAD). We then apply the same Δf to the Doppler shift of the I and Q samples containing the echo.

3. Observations

Figure 1 upper left panel shows the RTI plot for this experiment. RAX crossed loci-of-perpendicularity for altitudes 300 (F region), 200, and 100 km (E region) at times approximately 175, 205 and 235 seconds into the experiment. Echoing occurred between the times 200–250s. The echoes arrived 330ms after the arrival of the direct pulse, corresponding to E-region scattering altitudes.

Figure 4 shows the echo power at 90ms ACF lag (red line) and the echo Doppler velocity (blue line) computed from the same lag. The green line shows the power originally computed from the I and Q samples. Note that since the correlation time of UHF coherent scatter is on the order of 1ms (Hall and Moorcroft, 1988), the echo power computed from the ACF lag at 90ms is very well representative of the actual power. For the transmitted pulse of 100 us, the power from the ACF lag of 90 us has a time resolution of 10us, corresponding to an altitude resolution of 3 km.

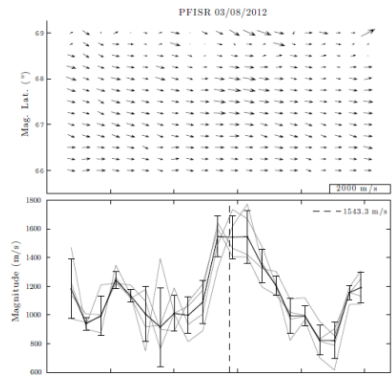


Figure 3: PFISR measurements of F region ion drift (top panel). F region ion drift at the magnetic latitude of coherent scatter (bottom panel).

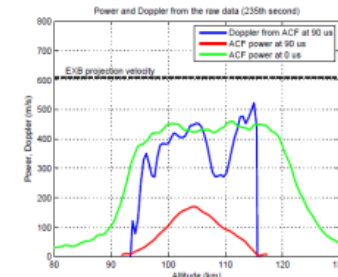


Figure 4: Raw echo intensity (green line), altitude-resolved intensity (red line) and Doppler velocity (blue line) as a function of altitude for the 235th second into the experiment (a vertical cut through the peak intensity in Figure 3).

Phase velocity. As seen in Figure 4, unlike the case of backscatter from the F region, auroral E-region coherent echoes do not exhibit Doppler shifts that are proportional to the line-of-sight convection speed in the scattering volume. The dashed horizontal line in Figure 4 shows the EXB drift projection velocity (~610 m/s) on the Bragg wavevector. The measured Doppler velocities of 300–400 m/s are lower than the dashed line, implying the saturation of the phase speeds. For this experiment, the EXB drift was measured to be 1543 m/s and was mostly uniform in latitude (see Figure 6). According to Nielsen and Schlegel [1985], the formula for the ion acoustic speed at 105 km is $C_s = 300 + 0.0011(\text{EXB}/B_2)$, which yields 562 m/s for the measured EXB drift. Moreover, the flow angle was 54 for the Bragg wavevector corresponding to the satellite position at the 235th second into the experiment. Combining these numbers, $C_s \cos \theta$ yields 328 m/s. Furthermore, we can estimate a collisional ion drift $V_i = E_{\text{eq}}/\mu_{\text{ion}}$ using an electric field $E = 84 \text{ mV/m}$ (corresponding to the EXB drift) and a collision frequency $\mu = 1000 \text{ s}^{-1}$, which yields $V_i = 268 \text{ m/s}$. Adding the projection of V_i on the Bragg wavevector (156 m/s) to $C_s \cos \theta$ yields 484 m/s, which is in excellent agreement with the measured Doppler velocity of 450 m/s for the altitude of 105 km.

Magnetic aspect angle distribution. Assuming coherent echoes originate inside the narrow ISR beam, we calculate echo altitude and magnetic aspect angle from echo delay. We have mapped the echo intensity to altitude and contours of magnetic aspect angle for the two crossing of the loci-of-perpendicularity as shown in Figure 5. Note that accurate timing of radar data acquisition is critical. For this experiment, 1 second of error corresponds to -0.15° aspect error. Although GPS was not operated for this experiment, we were able to determine the RAX clock to a precision of microseconds using direct PFISR pulses. The clock was ahead 4.66 seconds. As seen in Figure 5, after adjusting the experimental data, we find that echoing occurred when the scattering was perpendicular to B.

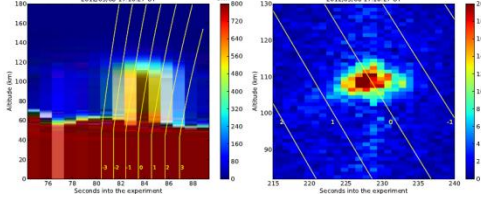


Figure 5: Radar echoes mapped to altitude and aspect angle/time coordinates for the first and second crossing of the loci of perp.

The 2nd crossing provided the best aspect angle resolution (RHS of Figure 5). The width of the aspect angle distribution is -0.5° , which is comparable to the radar beam width. To resolve the distribution to a better precision, one has to de-convolve the radar beam from the measurements. To do so, we first modeled the PFISR radar beam as in Figure 1 and then iterated a E region profiles of (1) backscatter intensity (2) aspect sensitivity and (3) mean aspect angle until the output of the forward model best fits the measurements corresponding to the altitude range 100–115 km. Figure 6 shows the modeled PFISR beam shape and the output of the forward model, which agrees remarkably well with the measurement shown in Figure 5 RHS.

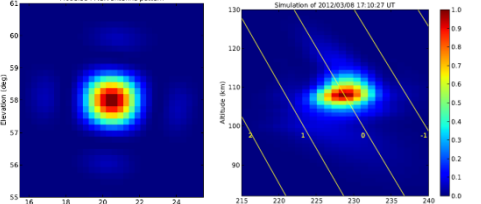
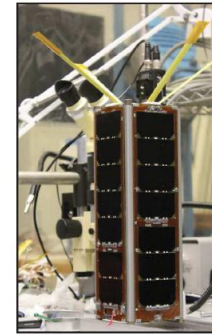


Figure 6: Modeled radar beam (left) and the output of the best fit model.



4. Summary

The best-fit profiles of backscatter intensity, aspect width and mean aspect angle shown in Figure 7 provide the highest resolution radar estimates of auroral irregularities so far. Furthermore, the unusually high electric field of 80 mV/m makes this a particularly interesting event. Our findings can be summarized as follows:

- (1) The echoes are only observed when the line-of-sight electron drift speed exceeds a threshold speed close to C_s . We have run 23 natural irregularity experiments and detected echoes only when the F region ion drift was 700, 1000 and 1600 m/s, all exceeding the threshold (500 m/s) for the Farley-Buneman instability.
- (2) The phase velocity is given by the empirical formula $C_s \cos \theta$.
- (3) UHF backscatter is confined to the altitude range of 105–112 km (3 dB points).
- (4) The radar echoes are highly aspect sensitive, with RMS aspect angles between 0.1° – 0.4° , which is also the range reported by *Kudeki and Farley* [1989] for equatorial E region irregularities. Using the upper value (0.4°), the power fall of 10 dB would occur within $\sim 1.3^\circ$, which is inline with the Hall and Moorcroft [1988] UHF measurements (power fall of 10 dB occurs within $1-2^\circ$). However, the surprising observations here are that (1) the electric field (80 mV/m) for the present experiment is much stronger than those reported by previous authors and therefore we expected RMS aspect angle width to be much larger, and (2) at 110 km altitude where the most electron heating is expected, the aspect angle is -0.2° , much narrower than expected.
- (5) The mean aspect angle does not favor 0.5° as predicted by the linear theory. In fact, it is single peaked and it varies between 0.6° at 100km to -0.4° at -115 km . A rough estimate shows that if a narrow sheet of electrojet Hall current generates 550 nT perturbation on the ground, the magnetic field immediately above and below this current will be bent by 550 nT as well. Considering about 50,000 nT total magnetic field, the resulting perturbation will bend the field by about 0.5° , inline with our observations.

In conclusion, at 110 km and at -80 mV/m electric field, FAI are field aligned with within $0.1-0.2^\circ$, well narrower than expected. Even considering that the RMS perpendicular wave electric field is on the order of the background electric field (80 mV/m), the corresponding parallel electric field will be between 0.13–0.27 mV/m. Electron plasma heating models show that about 1 mV/m parallel electric field is needed to heat the electron to observed temperatures of 1500 K for 80 mV/m at 110 km altitude. Therefore, contrary to current understanding (St. Maurice and Schlegel 1982, Miik and Dimant, 2003), the meter-scale waves at 110 km do not seem to have sufficient parallel electric fields to heat the electrons to the observed temperatures.

Bahcivan and Cosgrove [2010] proposed that parallel electric fields associated with long wavelength waves in the presence of vertical electron density gradients would be sufficient to heat the electrons. The results presented here therefore strongly suggest a shift of focus from meter scale waves to longer wavelengths to explain plasma heating in the auroral electrojet.

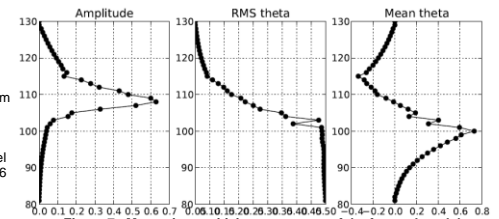


Figure 7: Magnetic sensitivity parameters of the forward model.

REFERENCES

- Cutler, J., and H. Bahcivan, The radio aurora explorer: A mission overview, AIAA Journal of Spacecraft and Rockets, accepted, 2012
- Bahcivan, H., J. Cutler, M. Bennett, B. Kampke, J. Springman, J. Buoncicore, M. Nicolls, and R. Doe, First measurements of radar coherent scatter by the Radio Aurora Explorer CubeSat, Geo. Res. Lett., 39, L14101, s PP, doi:10.1029/2012GL052249, 2012.
- Bahcivan, H., and J. Cutler, Radio Aurora Explorer: Mission science and radar system, Radio Sci., pp. doi:10.1029/2011RS004817, 2012.

Acknowledgements

RAX was developed under National Science Foundation grant ATM-0121483 to SRI International and the University of Michigan. PFISR operations and maintenance is supported by NSF cooperative agreement ATM-0608577 to SRI International.